Mathematical Study of Laminar Boundary Layer Flow and Heat Transfer of Tangenthyperbolic Fluid Pasta Vertical Porous Plate with Biot Number Effects

V. Ramachandra Prasad[1], S. Abdul Gaffar[2] and O. Anwar Bég[3]

[1] *Department of Mathematics, Madanapalle Institute of Technology and Science, Madanapalle-517325, India*
[2]*Department of Mathematics, Salalah College of Technology, Salalah, Oman*
[3] *Gort Engovation Research (Aerospace), 15 Southmere Avenue, Great Horton, Bradford, BD7 3NU, West Yorkshire, UK.*

†*Corresponding Author Email:* rcpmaths@gmail.com

ABSTRACT

In this article, we investigate the nonlinear steady boundary layer flow and heat transfer of an incompressible Tangent Hyperbolicnon-Newtonian fluid from a vertical porous plate. The transformed conservation equations are solved numerically subject to physically appropriate boundary conditions using a second-order accurate implicit finite-difference Keller Box technique. The numerical code is validated with previous studies. The influence of a number of emerging non-dimensional parameters, namely the Weissenberg number (W_e), the power law index (n), Prandtl number (Pr), Biot number (γ), and dimensionless local suction parameter(ξ)on velocity and temperature evolution in the boundary layer regime are examined in detail. Furthermore the effects of these parameters on *surface heat transfer rate* and *local skin friction* are also investigated. Validation with earlier *Newtonian* studies is presented and excellent correlation achieved. It is found that velocity, Skin friction and Nusselt number (heat transfer rate) are reduced with increasing Weissenberg number (W_e), whereas, temperature is enhanced. Increasing power law index (n) enhances velocity and Nusselt number (heat transfer rate) but temperature and Skin friction decrease. An increase in the Biot number (γ) is observed to enhance velocity, temperature, local skin friction and Nusselt number. An increasing Prandtl number, Pr, is found to decrease both velocity, temperature and skin friction but elevates heat transfer rate (Nusselt number). The study is relevant to chemical materials processing applications.

Keywords: Non-newtonian fluid; Tangent hyperbolic fluid; Boundary layers; Skin friction; Nusselt number; Weissenberg number; The power law index; Biot number.

NOMENCLATURE

B_0	constant Magnetic Field Intensity		α	thermal diffusivity
C_f	skin friction coefficient		η	dimensionless radial coordinate
f	non-dimensional stream function		μ	dynamic viscosity
Gr	Grashof number		ν	kinematic viscosity
g	acceleration due to gravity		θ	non-dimensional temperature
k	thermal conductivity of fluid		ρ	density of non-Newtonian fluid
n	power law index		ξ	local suction parameter
Nu	local Nusselt number		ψ	dimensionless stream function
Pr	Prandtl number		γ	Biot number
T	temperature of the fluid		Γ	time dependent material constant
u, v	non-dimensional velocity components along the x- and y- directions, respectively		Π	second invariant strain tensor
V	velocity vector		**Subscripts**	
V_0	transpiration velocity		w	surface conditions on plate (wall)
W_e	Weissenberg number		∞	free stream conditions
x	stream wise coordinate			
y	transverse coordinate			

1. INTRODUCTION

The dynamics of non-Newtonian fluids has been a popular area of research owing to ever-increasing applications in chemical and process engineering. Examples of such fluids include coal-oil slurries, shampoo, paints, clay coating and suspensions, grease, cosmetic products, custard, physiological liquids (blood, bile, synovial fluid) etc. The classical equations employed in simulating Newtonian viscous flows i.e. the Navier–Stokes equations fail to simulate a number of critical characteristics of non-Newtonian fluids. Hence several constitutive equations of non-Newtonian fluids have been presented over the past decades. The relationship between the shear stress and rate of strain in such fluids are very complicated in comparison to viscous fluids. The viscoelastic features in non-Newtonian fluids add more complexities in the resulting equations when compared with Navier–Stokes equations. Significant attention has been directed at mathematical and numerical simulation of non-Newtonian fluids. Recent investigations have implemented, respectively the Casson model (2013), second-order Reiner-Rivlin differential fluid models (2013), power-law nanoscale models (2013), Eringen micro-morphic models (2011) and Jefferys viscoelastic model (2013).

Convective heat transfer has also mobilized substantial interest owing to its importance in industrial and environmental technologies including energy storage, gas turbines, nuclear plants, rocket propulsion, geothermal reservoirs, photovoltaic panels etc. The convective boundary condition has also attracted some interest and this usually is simulated via a Biot number in the wall thermal boundary condition. Recently, Ishak (2010) discussed the similarity solutions for flow and heat transfer over a permeable surface with convective boundary condition. Aziz (2009) provided a similarity solution for laminar thermal boundary layer over a flat surface with a convective surface boundary condition. Aziz (2010) further studied hydrodynamic and thermal slip flow boundary layers with an iso-flux thermal boundary condition. The buoyancy effects on thermal boundary layer over a vertical plate subject a convective surface boundary condition was studied by Makinde and Olanrewaju (2010). Further recent analyses include Makinde and Aziz (2010). Gupta *et al.* (2013) used a variational finite element to simulate mixed convective-radiative micropolar shrinking sheet flow with a convective boundary condition. Makinde *et al.* (2012) studied cross diffusion effects and Biot number influence on hydromagnetic Newtonian boundary layer flow with homogenous chemical reactions and MAPLE quadrature routines. Bég *et al.* (2013) analyzed Biot number and buoyancy effects on magnetohydrodynamic thermal slip flows. Subhashini *et al.* (2011) studied wall transpiration and cross diffusion effects on free convection boundary layers with a convective boundary condition.

Convective boundary-layer flows are often controlled by injecting or withdrawing fluid through a porous bounding heat surface. This can lead to enhanced heating or cooling of the system and can help to delay the transition from laminar to turbulent flow. The case of uniform suction and blowing through an isothermal vertical wall was treated first by Sparrow and Cess (1961); they obtained a series solution which is valid near the leading edge. This problem was considered in more detail by Merkin (1972), who obtained asymptotic solutions, valid at large distances from the leading edge, for both the suction and blowing. Using the method of matched asymptotic expansion, the next order corrections to the boundary-layer solutions for this problem were obtained by Clarke (1973), who extended the range of applicability of the analyses by not invoking the usual Boussinesq approximation. The effect of strong suction and blowing from general body shapes which admit a similarity solution has been given by Merkin (1975). A transformation of the equations for general blowing and wall temperature variations has been given by Vedhanayagam *et al.* (1980). The case of a heated isothermal horizontal surface with transpiration has been discussed in some detail first by Clarke and Riley (1975, 1976) and then more recently by Lin and Yu (1988). Hossain *et al.* (2001) studied the effect of radiation on free convection flow with variable viscosity from a vertical porous plate.

An interesting non-Newtonian model developed for chemical engineering systems is the Tangent Hyperbolic fluid model. This rheological model has certain advantages over the other non-Newtonian formulations, including simplicity, ease of computation and physical robustness. Furthermore it is deduced from kinetic theory of liquids rather than the empirical relation. Several communications utilizing the Tangent Hyperbolic fluid model have been presented in the scientific literature. There is no single non-Newtonian model that exhibits all the properties of non-Newtonian fluids. Among several non-Newtonian fluids, hyperbolic tangent model is one of the non-Newtonian models presented by Popand Ingham (2001). Nadeem *et al.* (2009) made a detailed study on the peristaltic transport of a hyperbolic tangent fluidin an asymmetric channel. Nadeem and Akram (2011) investigated the peristaltic flow of a MHD hyperbolic tangent fluid in a vertical asymmetric channel with heat transfer. Akram and Nadeem (2012) analyzed the influence of heat and mass transfer on the peristaltic flow of a hyperbolic tangent fluid in an asymmetric channel. Very recently, Akbar *et al.* (2013) analyzed the numerical solutions of MHD boundary layer flow of tangent hyperbolic fluid on a stretching sheet.

The objective of the present study is to investigate the laminar boundary layer flow and heat transfer of a *Tangent Hyperbolic* non-Newtonian fluid past a vertical porous plate. The non-dimensional equations with associated dimensionless boundary conditions constitute a highly nonlinear, coupled two-point boundary value problem. Keller's implicit finite difference "box" scheme is

implemented to solve the problem (2012). The effects of the emerging thermophysical parameters, namely *the Weissenberg number (W_e), power law index (n),Biot number (γ) and Prandtl number (Pr),* on the velocity, temperature, skin friction number, and heat transfer rate (local Nusselt number) characteristics are studied. The present problem has to the authors' knowledge not appeared thus far in the scientific literature and is relevant to polymeric manufacturing processes in chemical engineering.

2. NON-NEWTONIAN CONSTITUTIVE TANGENT HYPERBOLIC FLUID MODEL

In the present study a subclass of non-Newtonian fluids known as the *Tangent Hyperbolic fluid* is employed owing to its simplicity. The Cauchy stress tensor, in the*Tangent Hyperbolic* non-Newtonian fluid [24] takes the form:

$$\bar{\tau} = \left[\mu_\infty + (\mu_0 + \mu_\infty)\tanh\left(\Gamma\bar{\dot{\gamma}}\right)^n \right]\bar{\dot{\gamma}} \tag{1}$$

where $\bar{\tau}$is extra stress tensor, μ_∞ is the infinite shear rate viscosity, μ_0 is the zero shear rate viscosity, Γ is the time dependent material constant, n is the power law index i.e. flow behaviour index and $\bar{\dot{\gamma}}$is defined as

$$\bar{\dot{\gamma}} = \sqrt{\frac{1}{2}\sum_i\sum_j \bar{\dot{\gamma}}_{ij}\bar{\dot{\gamma}}_{ji}} = \sqrt{\frac{1}{2}\Pi}, \tag{2}$$

Where $\Pi = \frac{1}{2}tr\left(gradV + \left(gradV\right)^T\right)^2$. We consider Eqn. (1), for the case when $\mu_\infty = 0$ because it is not possible to discuss the problem for the infinite shear rate viscosity and since we considering tangent hyperbolic fluid that describing shear thinning effects so $\Gamma\bar{\dot{\gamma}} < 1$. Then Eqn. (1) takes the form

$$\bar{\tau} = \mu_0\left[\left(\Gamma\bar{\dot{\gamma}}\right)^n\right]\bar{\dot{\gamma}} = \mu_0\left[\left(1 + \Gamma\bar{\dot{\gamma}} - 1\right)^n\right]\bar{\dot{\gamma}}$$

$$= \mu_0\left[1 + n\left(\Gamma\bar{\dot{\gamma}} - 1\right)\right]\bar{\dot{\gamma}} \tag{3}$$

The introduction of the appropriate terms into the flow model is considered next. The resulting boundary value problem is found to be well-posed and permits an excellent mechanism for the assessment of rheological characteristics on the flow behaviour.

3. MATHEMATICAL FLOW MODEL

The steady, laminar, two-dimensional, incompressible boundary layer flow and heat transfer of a Tangent Hyperbolic fluid past a vertical porous plate is considered, as illustrated in Fig. 1. Both the plate and Tangent Hyperbolic fluid are maintained initially at the same temperature. Instantaneously they are raised to a temperature T_w $> T_\infty$, the ambient temperature of the fluid which remains unchanged. In line with the approach of Yih (2000) and introducing the boundary layer approximations, the equations for *mass, momentum, and energy,* can be written as follows:

$$\frac{\partial u}{\partial x} + \frac{\partial v}{\partial y} = 0 \tag{4}$$

$$u\frac{\partial u}{\partial x} + v\frac{\partial u}{\partial y} = \nu(1-n)\frac{\partial^2 u}{\partial y^2} +$$
$$\sqrt{2}\nu n\Gamma\frac{\partial u}{\partial y}\frac{\partial^2 u}{\partial y^2} + g\beta(T - T_\infty) \tag{5}$$

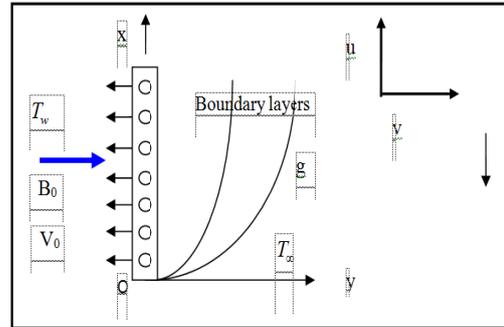$$u\frac{\partial T}{\partial x} + v\frac{\partial T}{\partial y} = \alpha\frac{\partial^2 T}{\partial y^2} \tag{6}$$

Fig. 1. Physical Model and Coordinate System.

where u and v are the velocity components in the x - and y- directions respectively, is the $\nu = \mu/\rho$ kinematic viscosity of the Tangent Hyperbolic fluid, β is the coefficient of thermal expansion, α is the thermal diffusivity, T is the temperature, ρ is the density of the fluid. The Tangent Hyperbolic fluid model therefore introduces a *mixed* derivative (second order, first degree) into the momentum boundary layer equation (5). The non-Newtonian effects feature in the shear terms only of eqn. (5) and not the convective (acceleration) terms. The third term on the right hand side of eqn. (5) represents the *thermal buoyancy force* and couples the velocity field with the temperature field equation (6).

At $y = 0$, $u = 0$, $v = 0$, $-k\frac{\partial T}{\partial y} = h_w(T_w - T)$

As $y \to \infty$, $u \to 0$, $T \to T_\infty$ \tag{7}

Here T_∞ is the free stream temperature, k is the thermal conductivity, h_w is the convective heat transfer coefficient, T_w is the convective fluid temperature. The stream function ψ is defined by

$u = \dfrac{\partial \psi}{\partial y}$ and $v = -\dfrac{\partial \psi}{\partial x}$, and therefore, the continuity equation is automatically satisfied. In order to render the governing equations and the boundary conditions in dimensionless form, the following non-dimensional quantities are introduced.

$$\xi = \frac{V_0 x}{v} Gr_x^{-1/4}, \eta = \frac{y}{x} Gr_x^{1/4}, \theta(\xi,\eta) = \frac{T - T_\infty}{T_w - T_\infty},$$

$$\psi = 4v\sqrt[4]{Gr_x}\left(f(\xi,\eta) + \frac{1}{4}\xi \right), \quad \Pr = \frac{v}{\alpha}$$

$$W_e = \frac{4\sqrt{2}\, v \Gamma Gr_x^{3/4}}{x^2}, Gr = \frac{g\beta(T_w - T_\infty)x^3}{4v^2} \tag{8}$$

All terms are defined in the nomenclature. In view of the transformation defined in eqn. (8), the boundary layer eqns. (5)-(7) are reduced to the following coupled, nonlinear, dimensionless partial differential equations for momentum and energy for the regime:

$$(1-n)f''' + (3f + \xi)f'' - 2(f')^2$$
$$+ nW_e f''f''' + \theta = \xi\left(f'\frac{\partial f'}{\partial \xi} - f''\frac{\partial f}{\partial \xi} \right) \tag{9}$$

$$\frac{\theta''}{\Pr} + (3f + \xi)\theta' = \xi\left(f'\frac{\partial \theta}{\partial \xi} - \theta'\frac{\partial f}{\partial \xi} \right) \tag{10}$$

The transformed dimensionless boundary conditions are:

$$At \quad \eta = 0, \quad f = 0, \quad f' = 0, \quad \theta = 1 + \frac{\theta'}{\gamma}$$

$$As \quad \eta \to \infty, \quad f' \to 0, \quad \theta \to 0 \tag{11}$$

Here primes denote the differentiation with respect to η and $\gamma = \dfrac{xh_w}{k} Gr_x^{-1/4}$ is the Biot number. The wall thermal boundary condition in (11) corresponds to convective cooling. The skin-friction coefficient (shear stress at the plate surface) and Nusselt number (heat transfer rate) can be defined using the transformations described above with the following expressions.

$$\frac{1}{4} Gr^{-3/4} C_f = (1-n)f''(\xi,0) + \frac{n}{2}W_e\left(f''(\xi,0)\right)^2 \tag{12}$$

$$Gr^{-1/4} Nu = -\theta'(\xi,0) \tag{13}$$

In the vicinity of the lower stagnation point, $\xi\sim 0$ and the boundary layer equations (9) – (10) contract to a system of ordinay differential equations:

$$(1-n)f''' + 3ff'' - 2(f')^2 + nW_e f''f''' + \theta = 0 \tag{14}$$

$$\frac{\theta''}{\Pr} + 3f\theta' = 0 \tag{15}$$

The general model is solved using a powerful and unconditionally stable finite difference technique introduced by Keller (1978). The Keller-box method has a second order accuracy with arbitrary spacing and attractive extrapolation features.

4. NUMERICAL SOLUTION WITH KELLER BOX IMPLICT METHOD

The Keller-Box implicit difference method is implemented to solve the nonlinear boundary value problem defined by eqns. (9)–(10) with boundary conditions (11). This technique, despite recent developments in other numerical methods, remains a powerful and very accurate approach for parabolic boundary layer flows. It is unconditionally stable and achieves exceptional accuracy (1978). Recently this method has been deployed in resolving many challenging, multi-physical fluid dynamics problems. These include hydromagnetic Sakiadis flow of non-Newtonian fluids (2009), nanofluid transport from a stretching sheet (2011), radiative rheological magnetic heat transfer (2009), water hammer modelling (2005), porous media convection (2008) and magnetized viscoelastic stagnation flows (2009). The Keller-Box discretization is fully coupled at each step which reflects the physics of parabolic systems – which are also fully coupled. Discrete calculus associated with the Keller-Box scheme has also been shown to be fundamentally different from all other mimetic (physics capturing) numerical methods, as elaborated by Keller [31]. The Keller Box Scheme comprises four stages.

1) Reduction of the Nth order partial differential equation system to N first order equations.

2) Finite Difference Discretization.

3) Quasilinearization of Non-Liner Keller Algebraic Equations.

4) Block-Tridiagonal Elimination of Linear Keller Algebraic Equations.

5. NUMERICAL RESULTS AND INTERPRETATION

Comprehensive solutions have been obtained and are presented in Tables 1-4 and Figs. 2 - 7. The numerical problem comprises two independent variables (ξ, η), two dependent fluid dynamic variables (f, θ) and five thermo-physical and body force control parameters, namely, W_e, n, γ, Pr, ξ. The following default parameter values i.e. $W_e = 0.3$, n = 0.3, $\gamma = 0.2$, Pr = 0.71, $\xi = 1.0$ are prescribed (unless otherwise stated). Furthermore the influence of local suction parameter on heat transfer characteristics is also investigated.

In Table 1, we present the influence of the Weissenberg number (W_e) on the Skin friction and heat transfer rate, along with a variation in ξ. Increasing W_e is found to reduce the Skin friction. For large values of W_e, the skin friction is negative. And increasing W_e, also reduces the heat transfer

Table 1 Values of C_f and *Nu* for different W_e and ξ(Pr = 0.71, n = 0.3, γ = 0.2)

W_e	$\xi = 1.0$		$\xi = 2.0$		$\xi = 3.0$	
	C_f	*Nu*	C_f	*Nu*	C_f	*Nu*
0.0	1.1596	0.2846	0.8958	0.4861	0.6109	0.7205
0.5	1.0685	0.2842	0.8380	0.4860	0.5833	0.7204
1.0	0.9897	0.2839	0.7873	0.4657	0.5583	0.6995
5.0	0.5871	0.2815	0.5150	0.4415	0.4107	0.6733
10.0	0.3167	0.2804	0.3108	0.4211	0.2959	0.6523
15.0	0.1436	0.2790	0.1333	0.3994	0.1267	0.6262
20.0	0.0026	0.2780	-0.0084	0.3777	-0.0021	0.6051
25.0	-0.0813	0.2771	-0.0800	0.3550	-0.1077	0.5790

Table 2 Values of C_f and *Nu* for different n and ξ(Pr = 0.71, W_e = 0.3, γ = 0.2)

n	$\xi = 1.0$		$\xi = 2.0$		$\xi = 3.0$	
	C_f	*Nu*	C_f	*Nu*	C_f	*Nu*
0.0	1.2047	0.2803	0.8979	0.4856	0.6105	0.7204
0.1	1.1783	0.2816	0.8898	0.4857	0.6071	0.7204
0.2	1.1454	0.2829	0.8780	0.4859	0.6006	0.7205
0.3	1.1032	0.2844	0.8602	0.4860	0.5940	0.7205
0.4	1.0460	0.2859	0.8328	0.4863	0.5812	0.7205
0.5	0.9650	0.2876	0.7881	0.4865	0.5596	0.7206
0.6	0.8433	0.2893	0.7122	0.4868	0.5209	0.7206
0.7	0.6506	0.2912	0.5776	0.4870	0.4477	0.7207
0.8	0.3322	0.2931	0.3311	0.4870	0.2999	0.7208

rate. Increasing ξ decreases the Skin friction. Whereas increasing ξ, increases the heat transfer rate.

Table2document results for the influence of *the power law index* (n) on skin friction and heat transfer rate along with a variation in ξ. It is observed that the increasing n, decreases Skin friction but increases heat transfer rate. Whereas increasing ξ, decreases the Skin friction but increases the Nusselt number.

Table 3 presents the influence of *the Biot number*

(γ) on skin friction and heat transfer rate along with a variation in ξ. It is observed that the increasing γ, increases both the Skin friction and heat transfer rate. And increasing ξ, decreases Skin friction but increases heat transfer rate.

Table 4 documents results for the influence of *the Prandtl number* (Pr) on skin friction and heat transfer rate along with a variation in ξ. It is observed that the increasing Pr, decelerates Skin friction but accelerates heat transfer rate. And increasing ξ, decreases the Skin friction but increases the heat transfer rate.

Table 3 Values of C_f and Nu for different γ and ξ(Pr = 0.71, n = 0.3, W_e = 0.3)

γ	ξ = 1.0		ξ = 2.0		ξ = 3.0	
	C_f	Nu	C_f	Nu	C_f	Nu
0.2	1.1032	0.2844	0.8602	0.4860	0.5940	0.7205
0.3	1.5940	0.4979	1.3561	0.8176	0.9738	1.2012
0.4	1.8114	0.6090	1.5815	0.9862	1.1585	1.4412
0.5	1.9350	0.6769	1.7106	1.0882	1.2676	1.5863
0.6	2.0150	0.7226	1.7945	1.1565	1.3396	1.6820
0.7	2.0710	0.7555	1.8533	1.2054	1.3905	1.7503
0.8	2.1124	0.7802	1.8968	1.2422	1.4295	1.8020
0.9	2.1443	0.7996	1.9315	1.2710	1.4592	1.8421
1.0	2.1693	0.8150	1.9580	1.2939	1.4827	1.8741

Table 4 Values of C_f and Nu for different Pr and ξ(W_e = 0.3, n = 0.3, γ = 0.2)

| Pr	ξ = 1.0		ξ = 2.0		ξ = 3.0	
	C_f	Nu	C_f	Nu	C_f	Nu
0.5	1.2598	0.2184	1.1381	0.3483	0.8359	0.5076
0.7	1.1098	0.2810	0.8711	0.4794	0.6024	0.7103
1.0	1.1718	0.5101	0.8242	0.9097	0.5620	1.3522
2.0	0.7641	0.9396	0.4174	1.8147	0.2817	2.7003
3.0	0.5353	1.3392	0.2775	2.7195	0.1895	4.0472
5.0	0.3212	2.3163	0.1637	4.5291	0.1090	6.7423
7.0	0.2268	3.2426	0.1139	6.3409	0.0748	9.4408
8.0	0.1969	3.7064	0.0981	7.2470	0.0638	10.7911
10.0	0.1543	4.6360	0.0752	9.0596	0.0478	13.4891

Figures 2(a) – 2(b) depict the velocity (f') and temperature (θ) distributions with increasing *Weissenberg number, We*. Very little tangible effect is observed in fig. 2a, although there is a very slight decrease in velocity with increase in *We*. Conversely, there is only a very slight increase in temperature magnitudes in Fig. 2(b) with a rise in *We*. The mathematical model reduces to the *Newtonian viscous flow model* as $W_e \to 0$ and $n \to 0$. The momentum boundary layer equation in this case contracts to the familiar equation for *Newtonian mixed convection* from a plate, viz.

$$f''' + (3f + \xi)f'' - 2f'^2 + \theta$$
$$= \xi\left(f'\frac{\partial f'}{\partial \xi} - f''\frac{\partial f}{\partial \xi}\right) \quad .$$

The thermal boundary layer equation (10) remains unchanged.

Figures 3(a) - 3(b) illustrates the effect of the *power law index, n,* on the velocity (f') and temperature (θ) distributions through the boundary layer regime. Velocity is increased with increasing *n*.
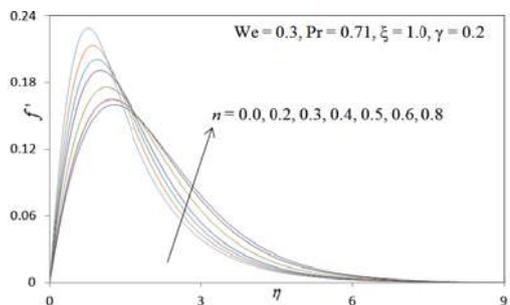
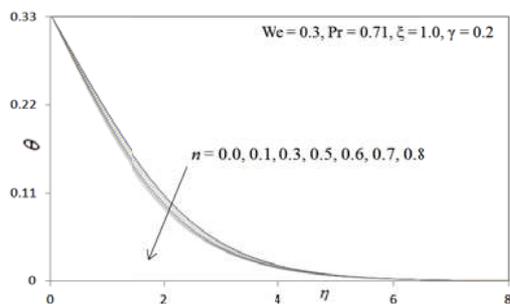Conversely temperature is consistently reduced with increasing values of *n*.
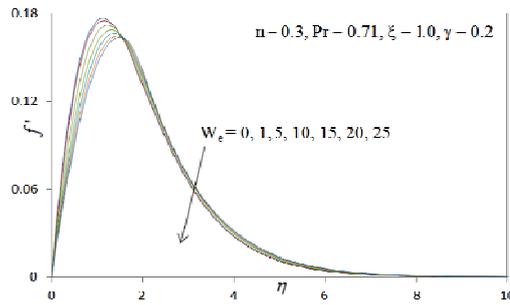
Fig. 2. (a) Influence of W_e on Velocity Profiles.
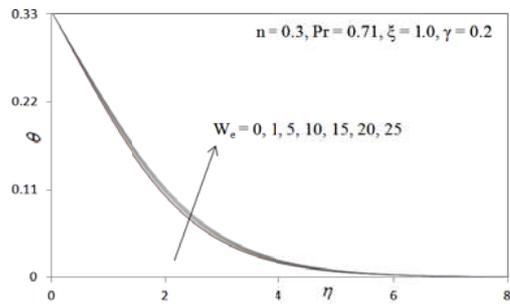
Fig. 2. (b) Influence of We on Temperature Profiles.
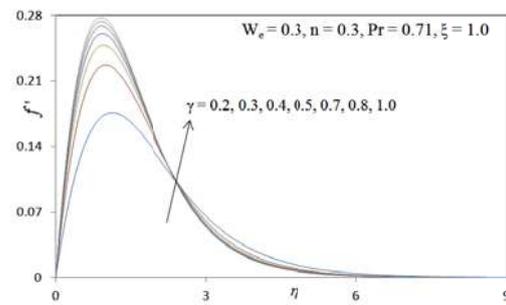

Fig. 3. (a) Influence of *n* on Velocity Profiles.

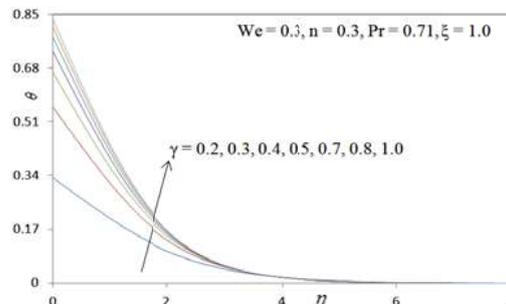

Fig. 3. (b) Influence of *n* on Temperature Profiles.

Figures 4(a) - 4(b) depict the evolution of velocity (f') and temperature (θ) functions with a variation in Biot number, γ. Dimensionless velocity component (fig. 4a) is considerably enhanced with increasing γ. In fig. 4b, an increase in Biot number is seen to considerably enhance temperatures

throughout the boundary layer regime. For $\gamma < 1$ i.e. small Biot numbers, the regime is frequently designated as being "thermally simple" and there is a presence of more uniform temperature fields inside the boundary layer and the plate solid surface. For $\gamma > 1$ thermal fields are anticipated to be non-uniform within the solid body. The Biot number effectively furnishes a mechanism for comparing the conduction resistance within a solid body to the convection resistance external to that body (offered by the surrounding fluid) for heat transfer. We also note that a Biot number in excess of 0.1, as studied in figs. 4a, b corresponds to a "thermally thick" substance whereas Biot number less than 0.1 implies a "thermally thin" material. Since γ is inversely proportional to thermal conductivity (k), as γ increases, thermal conductivity will be reduced at the plate surface and this will lead to a decrease in the rate of heat transfer from the boundary layer to within the plate, manifesting in a rise in temperature at the plate surface and in the body of the fluid- the maximum effect will be sustained at the surface, as witnessed in fig. 4b. However for a fixed wall convection coefficient and thermal conductivity, Biot number as defined in $\gamma = \dfrac{x h_w}{k} Gr^{-1/4}$ is also directly inversely proportional to the local Grashof (free convection) number. As local Grashof number increases generally the enhancement in buoyancy causes a deceleration in boundary layer flows [40 - 42]; however as Biot number increases, the local Grashof number must decreases and this will induce the opposite effect i.e. accelerate the boundary layer flow, as shown in fig. 4a.
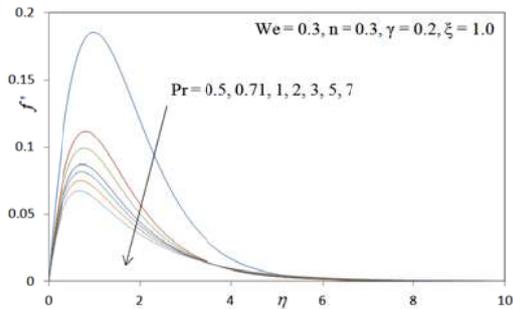

Fig. 4. (a) Influence of γ on Velocity Profiles.

Fig. 4. (b) Influence of γ on Temperature Profiles.

Figures 5(a) – 5(b) depicts the profiles for velocity

(f') and temperature (θ) for various values of Prandtl number, Pr. It is observed that an increase in the Prandtl number significantly decelerates the flow i.e., velocity decreases. And increasing Prandtl number is found to decelerate the temperature.
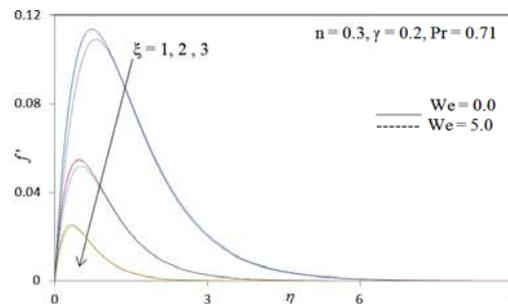

Fig. 5.(a) Influence of Pr on Velocity Profiles.
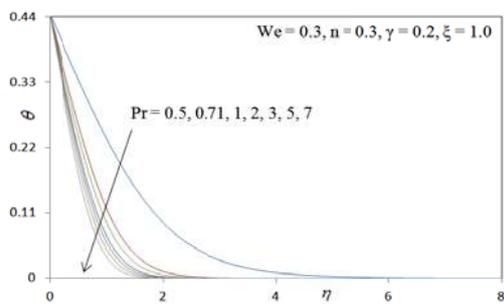
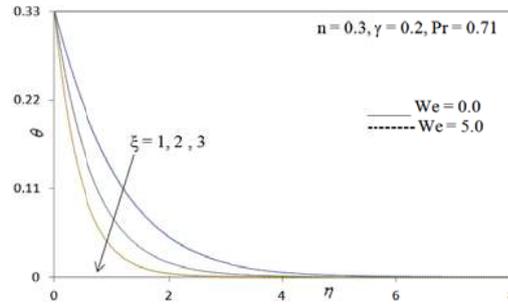**Fig. 5. (b) Influence of Pr on Temperature Profiles.**

Figures 6(a) – 6(b) depicts the velocity $\left(f'\right)$ and temperature (θ) distributions with radial coordinate, for various local suction parameter values, ξ along with the variation in the Weissenberg number (W_e). Clearly, from these figures it can be seen that as suction parameter ξ increases, the maximum fluid velocity decreases. This is due to the fact that the effect of the suction is to take away the warm fluid on the vertical plate and thereby decrease the maximum velocity with a decrease in the intensity of the natural convection rate. Fig. 6(b) shows the effect of the local suction parameter on the temperature profiles. It is noticed that the temperature profiles decrease with an increase in the suction parameter and as the suction is increased, more warm fluid is taken away and this the thermal boundary layer thickness decreases. It is also seen that an increase in W_e, the impedance offered by the fibers of the porous medium will increase and this will effectively decelerate the flow in the regime, as testified to by the evident decrease in velocities shown in fig. 6(a).

Figures 7(a) – 7(b) depict the velocity (f') and temperature (θ) distributions with radial coordinate, for various local suction parameter values, ξ along with the variation in the power law index (n).Clearly, from these figures it can be seen that as suction parameter ξ increases, the maximum fluid velocity decreases. This is due to the fact that the effect of the suction is to take away the warm fluid on the vertical plate and thereby decrease the maximum velocity with a decrease in the intensity of the natural convection rate. Fig. 7(b) shows the effect of the local suction parameter on the temperature profiles. It is noticed that the temperature profiles decrease with an increase in the suction parameter and as the suction is increased, more warm fluid is taken away and this the thermal boundary layer thickness decreases. It is also seen that an increase in *n*, the impedance offered by the fibers of the porous medium will increase and this will effectively decelerate the flow in the regime, as testified to by the evident decrease in velocities shown in fig. 7(a).

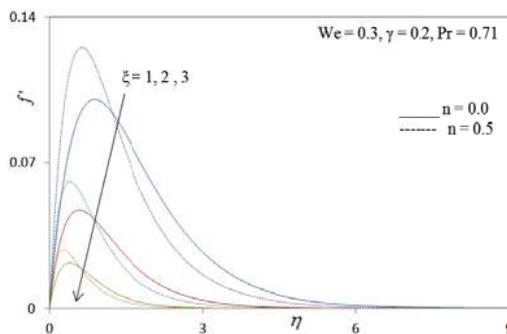**Fig. 6. (a) Influence of ξ and W_e on Velocity Profiles.**

Fig. 6. (b) Influence of ξ and W_e on Temperature Profiles.

6. CONCLUSIONS

Numerical solutions have been presented for the buoyancy-driven flow and heat transfer of Tangent Hyperbolic flow external to a vertical porous plate. The Keller-box implicit second order accurate finite difference numerical scheme has been utilized to efficiently solve the transformed, dimensionless velocity and thermal boundary layer equations, subject to realistic boundary conditions. Excellent correlation with previous studies has been demonstrated testifying to the validity of the present code. The computations have shown that:

1. Increasing Weissenberg number, W_e, reduces the velocity, skin friction (surface shear stress) and heat transfer rate, whereas it elevates temperature in the boundary layer.

2. Increasing power law index, *n*, increases the velocity and Nusselt number for all values of radial coordinate i.e., throughout the boundary layer regime whereas it depresses temperature and skin friction.

3. Increasing Biot number, γ, increases velocity, temperature, skin friction (surface shear stress) and heat transfer rate.

4. Increasing Prandtl number, Pr, decreases velocity, temperature and skin friction but increases heat transfer rate (Nusselt number).

5. Increasing transverse coordinate (ξ) along with increase in the Weissenberg number (W$_e$), generally decelerates the flow near the plate surface and reduces momentum boundary layer thickness and also reduces temperature and therefore decreases thermal boundary layer thickness in Tangent Hyperbolic non-Newtonian fluids.

6. Increasing transverse coordinate (ξ) along with increase in the power law index (n), generally decelerates the flow near the plate surface and reduces momentum boundary layer thickness and also reduces temperature and therefore decreases thermal boundary layer thickness in Tangent Hyperbolic non-Newtonian fluids.

Fig. 7. (a) Influence of ξ and on Velocity Profiles.
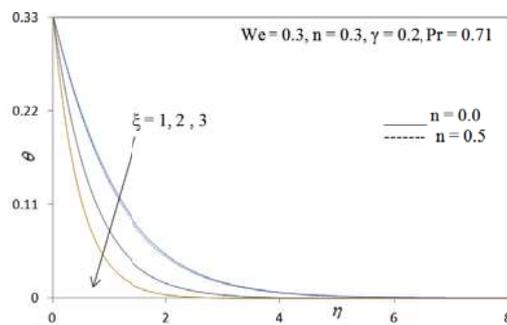
Fig. 7. (b) Influence of ξ and on Temperature Profiles.

Generally very stable and accurate solutions are obtained with the present finite difference code. The numerical code is able to solve nonlinear boundary layer equations very efficiently and therefore shows excellent promise in simulating transport phenomena in other non-Newtonian fluids.

REFERENCES

Akbar, N. S., S. Nadeem, R. U. Haq and Z. H. Khan (2013). Numerical solution of Magnetohydrodynamic boundary layer flow of tangent hyperbolic fluid towards a stretching sheet. *Indian J. Phys* 87 (11), 1121-1124.

Akram, S., N. Sohail (2012). Simulation of heat and mass transfer on peristaltic flow of hyperbolic tangent fluid in an asymmetric channel. *Int. J. Numer. Meth. Fluids.*

Anwar Bég, O., V. R. Prasad, B. Vasu, N. Bhaskar Reddy, Q. Li and R. Bhargava (2011). Free convection heat and mass transfer from an isothermal sphere to a micropolar regime with Soret/Dufour effects. *Int. J. Heat and Mass Transfer* 54, 9-18.

Anwar Bég, O., M. J. Uddin, M. M. Rashidi and N. Kavyani (2013). Double-diffusive radiative magnetic mixed convective slip flow with Biot number and Richardson number effects. *J. Engineering Thermophysics.*

Anwar, H. M., K. Khanafer and K. Vafai (2001). The effect of radiation on free convection flow with variable viscosity from a porous vertical plate. *Int. J. Therm. Sci* 40, 115-124.

Aziz, A. and A. Similarity (2009). solution for laminar thermal boundary layer over a flat plate with a convective surface boundary condition, *Comm.Non. Sci. Num. Sim*. 14(4), 1064–1068.

Aziz, A. (2010). Hydrodynamic and thermal slip flow boundary layers over a flat plate with constant heat flux boundary condition. *Comm. Non. Sci. Num. Sim*. 15, 573–580.

Chen, C. H. (2009). Magneto-hydrodynamic mixed convection of a power-law fluid past a stretching surface in the presence of thermal radiation and internal heat generation/absorption. *Int. J. Non-Linear Mechanics* 44, 596-603.

Chen, H. T. and C. K. Chen (1988). Natural convection of a non-Newtonian fluid about a horizontal cylinder and a sphere in a porous medium, *Int. Comm. Heat Mass Transfer* 15, 605–614.

Clarke, J. F. and N. Riley (1976). Free convection and the burning of a horizontal fuel surface. *Journal of Fluid Mechanics* 74, 415-431.

Clarke, J. F. and N. Riley (1975). Natural convection induced in a gas by the presence of a hot porous horizontal surface. *Q. J. Mech. Appl. Math*. 28, 373-396.

Clarke, J. F. (1973). Transpiration and natural convection: the vertical flat plate problem. *Journal of fluid Mechanics* 57, 45-61.

Gupta, D., L. Kumar, O. Anwar Bég and B. Singh (2013). Finite element simulation of mixed convection flow of micropolar fluid over a shrinking sheet with thermal radiation, *Proc. IMechE. Part E: J Process Mechanical*

Engineering.

Ishak, A. (2010). Similarity solutions for flow and heat transfer over a permeable surface with convective boundary condition, *Appl. Math. Comput.* 217, 837–842.

Keller, H. B. (1978). Numerical methods in boundary-layer theory. *Ann. Rev. Fluid Mech.* 10, 417-433

Kumari, M., G. Nath (2009). Steady mixed convection stagnation-point flow of upper convected Maxwell fluids with magnetic field. *Int. J. Nonlinear Mechanics* 44, 1048-1055.

Lin, H. T. and W. S. Yu (1988). Free convection on a horizontal plate with blowing and suction. *Transaction of ASME Journal of Heat Transfer* 110, 793-796.

Makinde, O. D., K. Zimba and O. Anwar Bég (2012). Numerical study of chemically-reacting hydromagnetic boundary layer flow with Soret/Dufour effects and a convective surface boundary condition. *Int. J. Thermal and Environmental Engineering* 4, 89-98.

Makinde, O. D., A. Aziz (2010). MHD mixed convection from a vertical plate embedded in a porous medium with a convective boundary condition. *Int. J. Therm. Sci.* 49, 1813–1820.

Makinde, O. D. and P. O. Olanrewaju (2010). Buoyancy effects on thermal boundary layer over a vertical plate with a convective surface boundary condition. *Trans. ASME J. Fluids Eng.* 4, 132.

Merkin, H. J. (1975). The effects of blowing and suction on free convection boundary layers. *International Journal of Heat Mass Transfer* 18, 237-244.

Merkin, J. H. (1972). Free convection with blowing and suction. *International Journal of Heat Mass Transfer* 15, 989-999.

Nadeem, S. and S. Akram (2011). Magnetohydrodynamic peristaltic flow of a hyperbolic tangent fluid in a vertical asymmetric channel with heat transfer. *Acta Mech. Sin.,* 27(2), 237–250.

Nadeem, S. and S. Akram (2009). Peristaltic transport of a hyperbolic tangent fluid model in an asymmetric channel. *ZNA 64, 559–567.*

Norouzi, M., M. Davoodi, O. Anwar Bég and A. A. Joneidi (2013). Analysis of the effect of normal stress differences on heat transfer in creeping viscoelastic Dean flow. *Int. J. Thermal Sciences* 69, 61-69.

Orhan, A. and A. Kaya (2008). Non-Darcian forced convection flow of viscous dissipating fluid over a flat plate embedded in a porous medium, *Transport in Porous Media* 73, 173-186.

POP, I. and D. B. INGHAM (2001). *Convective Heat Transfer: Mathematical and Computational Modelling of Viscous Fluids and Porous Media.*

Pergamon, Amsterdam, NewYork.

Potter, J. N. and N. Riley (1980). Free convection from a heated sphere at large Grashof number. *J. Fluid Mechanics* 100, 769-783.

Prasad, V. R., B. Vasu, O. Anwar Bég and D. R. Parshad (2012). Thermal radiation effects on magnetohydrodynamic free convection heat and mass transfer from a sphere in a variable porosity regime. *Comm. Nonlinear Science Numerical Simulation* 17, 654–671.

Prasad, V. R., B. Vasu, O. Anwar Bég and D. R. Parshad (2012). Thermal radiation effects on magnetohydrodynamic free convection heat and mass transfer from a sphere in a variable porosity regime. *Comm. Nonlinear Science Numerical Simulation* 17, 654–671.

Prhashanna, A. and R. P. Chhabra (2010). Free convection in power-law fluids from a heated sphere. *Chem. Eng. Sci.* 65, 6190-6205

Ramachandra, P. V., A. Subba Rao, N. Bhaskar Reddy, B. Vasu and O. Anwar Bég (2013). Modelling laminar transport phenomena in a Casson rheological fluid from a horizontal circular cylinder with partial slip. *Proc IMechE Part E: J Process Mechanical Engineering.*

Rashidi, M. M., M. Keimanesh, O. Anwar Bég and T. K. Hung (2011). Magneto-hydrodynamic biorheological transport phenomena in a porous medium: A simulation of magnetic blood flow control. *Int. J. Numer. Meth. Biomed. Eng.* 27(6), 805-821.

Sparrow, E. M. and R. D. Cess (1961). Free convection with blowing or suction. Journal of Heat Transfer 83, 387-396.

Subhas, Abel M., P. S. Datti and N. Mahesha (2009). Flow and heat transfer in a power-law fluid over a stretching sheet with variable thermal conductivity and non-uniform heat source. *Int. J. Heat Mass Transfer* 52, 2902-2913.

Subhashini, S. V, N. Samuel and I. Pop (2011). Double-diffusive convection from a permeable vertical surface under convective boundary condition. *Int. Commun. Heat Mass Transfer* 38 1183-1188.

Tripathi, D, S. K. Pandey and O. Anwar Bég (2013). Mathematical modelling of heat transfer effects on swallowing dynamics of viscoelastic food bolus through the human oesophagus. *Int. J. Thermal Sciences* 70, 41-53.

Uddin, M. J., N. H. M. Yusoff, O. Anwar Bég and A. I. Ismail (2013). Lie group analysis and numerical solutions for non-Newtonian nanofluid flow in a porous medium with internal heat generation. *Physica Scripta* 87, 2.

Vajravelu, K., K. V. Prasad, J. Lee, C. Lee, I. Pop and A. Rob (2011). Van Gorder, Convective heat transfer in the flow of viscous Ag–water and Cu–water nanofluids over a stretching surface. *Int. J. Thermal Sciences* 50, 843-851.

Vedhanayagam, M., R. A. Altenkirch and R. Eichhorn (1980). A transformation of the boundary layer equations for the free convection past a vertical flat plate with arbitrary blowing and suction wall temperature variations. *International Journal of Heat Mass Transfer* 23, 1286-1288.

Yih, K. A. (2000). Viscous and Joule Heating effects on non-Darcy MHD natural convection flow over a permeable sphere in porous media with internal heat generation. *International Communications in Heat and mass Transfer* 27(4), 591-600.

Zhang, Y. L. and K. Vairavamoorthy (2005). Analysis of transient flow in pipelines with fluid–structure interaction using method of lines. *Int. J. Num. Meth. Eng* 63, 1446-1460.